

Optical Fluorescence Tomography With The Equation Of Radiative Transfer For Molecular Imaging

Alexander D. Klose and Andreas H. Hielscher

Departs. of Biomedical Engineering & Radiology, Columbia University, ET351 Mudd Building,
MC 8904, 500 West 120th Street, New York, N.Y. 10027, USA

ABSTRACT

Optical fluorescence tomography recovers the spatial distribution of light emitting fluorophores inside a highly scattering medium. The quantification of a non-uniform quantum yield and fluorophore absorption distribution is of major interest in molecular imaging of biological tissue. We have developed a fluorescence image reconstruction code that is based on the particle transport equation. Since the algorithm does not rely on the diffusion approximation it promises to yield more accurate results in highly absorbing media or media with small geometries. We show that the code can be employed in a two-stage reconstruction process to obtain images of the fluorophore absorption and of the quantum yield.

Keywords: fluorescence tomography, molecular imaging, equation of radiative transfer, finite-difference method, discrete-ordinates method, image reconstruction, quantum yield

1. INTRODUCTION

Optical fluorescence methods play a prominent role in the fast advancing field of molecular imaging. The advent of many novel biochemical markers that can detect molecular processes that precede the development of diseases promise to bring about fundamental changes in medical practice and molecular imaging.¹⁻³ Molecular imaging makes use of fluorescent probes that emit light when attached to specific biological targets or when a specific biochemical environment is encountered. One can distinguish two mechanisms that lead to a change in fluorescence signal at certain sites in the body: (1) concentration changes of the fluorophore due to preferential uptake or washout at certain sites, and (2) fluorescence quenching which results in changes of the quantum yield.⁴

Most work in this area has been limited to direct imaging of fluorescent light that escapes the surface of small animals. In this case an exact localization of light-emitting sources inside the tissue is not possible. Therefore, several groups have started to develop tomographical image reconstruction schemes, that use measured fluorescence signals on the surface of the tissue to determine the spatial fluorescence distribution inside the tissue.⁵⁻¹³ For example Ntziachristos *et al* have developed an algorithm that images the concentration of fluorescence probes in mice.¹³

The majority of these tomographical imaging modalities are based on the diffusion model of light propagation in tissue.¹⁴⁻¹⁶ However, it is well known that the diffusion model is only an approximation to the more generally applicable equation of radiative transfer (ERT). The limits of the diffusion approximation have been well documented¹⁷⁻²⁰ such as for highly absorbing media and media with small geometries where boundary effects are dominating.

In this work we present an optical fluorescence image reconstruction model that is based on the ERT. We present results that show that our algorithm can recover the spatial distribution of the quantum yield and absorption properties of a fluorophore. To solve that image reconstruction problem we adapted a model-based iterative image reconstruction scheme that we have previously developed for non-fluorescent optical tomography (OT).²¹⁻²³

Further author information:

A.D.K.: E-mail: ak2083@columbia.edu, Telephone: 1 212 854 5868

A.H.H.: E-mail: ahh2004@columbia.edu, Telephone: 1 212 854 5080

2. THEORY

Currently, the most promising solution methods in OT are the so-called model-based iterative image reconstruction (MOBIIR) schemes. A MOBIIR scheme applied to OT reconstructs the distribution of the optical parameters inside a highly scattering medium using measurement data obtained on the surface of the medium.^{14–16, 21} This scheme consists of two major components: (1) a *forward model* for light propagation and (2) an *inverse model*. The forward model predicts the detector readings on the tissue boundary given a distribution of optical properties inside the medium. In contrast, the inverse model determines the optical parameters inside the tissue, given a set of detector readings and detector predictions on the boundary of the tissue (see figure (1)).

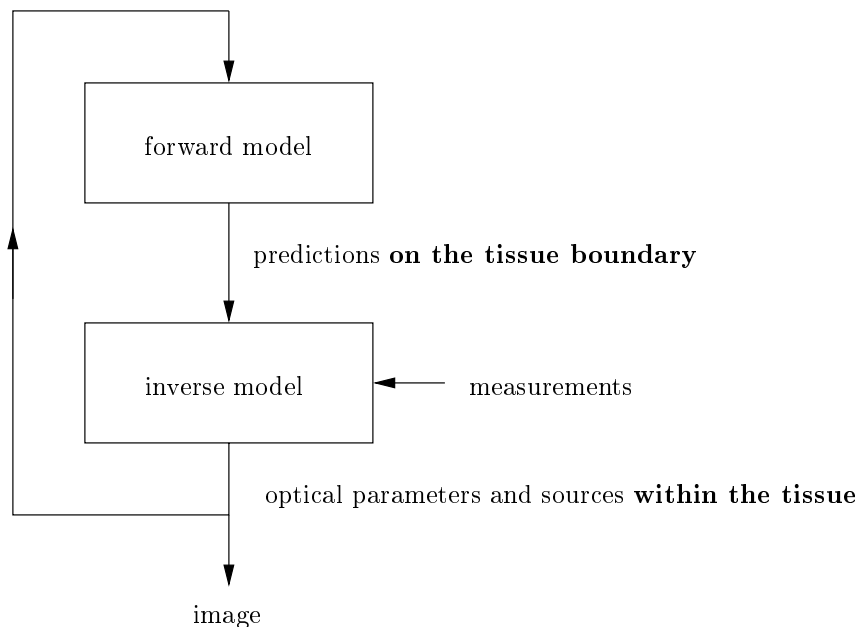


Figure 1. Components of the MOBIIR scheme in fluorescence OT for determining cross-sectional images of the optical parameters such as the fluorophore absorption and the quantum yield. The forward model for light propagation in tissue is iteratively employed to calculate detector predictions. The image is obtained by updating the optical parameters and sources within the inverse model.

The reconstruction process can be performed in two stages. First, the fluorophore absorption is reconstructed giving some information about the fluorophore uptake or fluorophore concentration inside the tissue. Second, the quantum yield distribution of the fluorophore is reconstructed that gives information about its biochemical environment and quenching processes.

2.1. Forward Model

The light transport in biological tissue is described by the equation of radiative transfer. A derivation of this equation is given by Duderstadt and Martin.²⁴ The ERT describes the transport of low energy photons through matter, such as human tissue, with absorbing and scattering properties. The three-dimensional time-independent ERT is given by:

$$\boldsymbol{\Omega} \cdot \nabla \psi(\mathbf{r}, \boldsymbol{\Omega}) + (\mu_a(\mathbf{r}) + \mu_s(\mathbf{r}))\psi(\mathbf{r}, \boldsymbol{\Omega}) = S(\mathbf{r}, \boldsymbol{\Omega}) + \mu_s(\mathbf{r}) \int_{4\pi} p(\boldsymbol{\Omega}, \boldsymbol{\Omega}')\psi(\mathbf{r}, \boldsymbol{\Omega}')d\boldsymbol{\Omega}'. \quad (1)$$

The fundamental quantity in radiative transport theory is the radiance $\psi(\mathbf{r}, \boldsymbol{\Omega})$, with units of $\text{Wcm}^{-2}\text{sr}^{-1}$, at the spatial position \mathbf{r} and unit direction $\boldsymbol{\Omega}$. Furthermore, the integral of the radiance $\psi(\mathbf{r}, \boldsymbol{\Omega})$ over all directions

Ω at one point \mathbf{r} yields the fluence $\phi(\mathbf{r})$ with units of Wcm^{-2} :

$$\phi(\mathbf{r}) = \int_{4\pi} \psi(\mathbf{r}, \Omega) d\Omega. \quad (2)$$

Other quantities besides the radiance ψ that are included in the ERT are the source term $S(\mathbf{r}, \Omega)$ with the unit $\text{Wcm}^{-3}\text{sr}^{-1}$, the scattering coefficient, $\mu_s(\mathbf{r})$, the absorption coefficient, $\mu_a(\mathbf{r})$, both given in units of cm^{-1} , and the scattering phase function $p(\Omega, \Omega')$ with units of sr^{-1} .

The light distribution originating from internal fluorescent sources can be described by a hierarchical system of two time-independent ERTs for the radiance $\psi(\mathbf{r}, \Omega)$. First, the light propagation caused by an external light source S^x at the excitation wavelength λ^x is calculated by the ERT

$$\Omega \cdot \nabla \psi^x + (\mu_a^{x \rightarrow} + \mu_a^{x \rightarrow m} + \mu_s^x) \psi^x = S^x + \mu_s^x \int_{4\pi} p(\Omega, \Omega') \psi^x(\Omega') d\Omega'. \quad (3)$$

The absorption coefficient $\mu_a^x(\mathbf{r})$ consists of the intrinsic absorption $\mu_a^{x \rightarrow}(\mathbf{r})$ of the tissue and the absorption $\mu_a^{x \rightarrow m}(\mathbf{r})$ due to the fluorochrome. The fluorophore absorption $\mu_a^{x \rightarrow m}(\mathbf{r}) = c(\mathbf{r}) \cdot \epsilon$ is linearly proportional to the fluorophore concentration $c(\mathbf{r})$ and the known fluorophore extinction coefficient ϵ .

The fluence distribution $\phi^x(\mathbf{r})$ excites a fluorochrome inside the tissue at position \mathbf{r} . The excited fluorophore with the quantum yield $\eta(\mathbf{r})$ constitutes an internal source $S^m(\mathbf{r}, \Omega) = \frac{1}{4\pi} \eta(\mathbf{r}) \mu_a^{x \rightarrow m}(\mathbf{r}) \phi^x(\mathbf{r})$ and emits light at the fluorescence wavelength λ^m . Furthermore, the emission source strength is directly proportional to the fluorophore concentration or the fluorophore absorption, respectively. The fluence distribution $\phi^m(\mathbf{r})$ of the fluorescent field is calculated by a second ERT (equation (4)) with the optical parameters $\mu_a^m(\mathbf{r})$ and $\mu_s^m(\mathbf{r})$ at the fluorescence wavelength λ^m :

$$\Omega \cdot \nabla \psi^m + (\mu_a^m + \mu_s^m) \psi^m = \frac{1}{4\pi} \eta \mu_a^{x \rightarrow m} \phi^x + \mu_s^m \int_{4\pi} p(\Omega, \Omega') \psi^m(\Omega') d\Omega'. \quad (4)$$

Both transport equations, equations (3) and (4), need to be solved numerically because no analytical solutions of the ERT are available for spatially heterogeneous media with finite geometrical boundaries. First, the direction Ω is replaced with a set of discrete ordinates Ω_k with *full level symmetry* by utilizing a *discrete ordinates* (S_N) method.^{25, 26} The integral in the ERT is approximated with a quadrature rule

$$\int_{4\pi} p(\Omega, \Omega') \psi(\Omega') d\Omega' \approx \sum_{k'=1}^K w_{k'} p(\Omega_k, \Omega_{k'}) \psi(\Omega_{k'}) \quad (5)$$

where w_k are appropriate weights²⁶ determined by full level symmetry of the ordinates. The total number of ordinates K is given by $K = \mathcal{N}(\mathcal{N} + 2)$ with \mathcal{N} the number of direction cosines of the S_N method.

The spatial derivatives are substituted with first-order finite differences approximations known as *step method*^{25, 26} or *upwind scheme*.²⁷ The discretized ERTs result in an algebraic system of equations

$$\mathbf{A}\psi = \mathbf{B}\psi + \mathbf{S} \quad (6)$$

with \mathbf{A} as the discretized streaming and collision operator, \mathbf{B} as the discretized integral operator, and \mathbf{S} as source term. By considering a *source iteration* (SI) mode^{25, 26} we recast that equation to

$$\mathbf{A}\psi^{n+1} = \mathbf{B}\psi^n + \mathbf{S} \quad (7)$$

and solve it for the radiance ψ^{n+1} with a *Gauss-Seidel* method in order to determine the predicted detector readings on the tissue boundary.

2.2. Inverse Model

The spatial distributions of optical parameters, $\mu_a^{x \rightarrow m}(\mathbf{r})$ and $\eta(\mathbf{r})$, are reconstructed by applying nonlinear optimization techniques to objective functions $\varphi(\mu_a^{x \rightarrow m})$ and $\varphi(\eta)$, which describe the difference between the measured m_d and predicted data p_d for all D source-detector pairs

$$\varphi \approx \sum_{d=1}^D \left(\frac{p_d - m_d}{m_d} \right)^2. \quad (8)$$

We minimize the objective function by using gradient-based optimization techniques. Gradient-based optimization techniques have been proven to be computationally efficient for large-scale problems^{28,29} such as in OT, where between 10^3 and 10^5 unknown optical parameters are common. These optimization techniques use the gradient $\nabla\varphi(\boldsymbol{\mu})$ and $\nabla\varphi(\boldsymbol{\eta})$ of the objective function for calculating a *search direction* $\mathbf{u}_k(\nabla\varphi)$ and a *step length* α_k to find a new update of optical parameters. An updating scheme determines, for example, a new estimate of the sequence $\{\boldsymbol{\eta}_k\}$ of quantum yields:

$$\boldsymbol{\eta}_{k+1} = \boldsymbol{\eta}_k + \alpha_k \mathbf{u}_k. \quad (9)$$

Therefore, calculating the new estimate $\boldsymbol{\eta}_{k+1}$ is broken up into two tasks:

- finding a proper step length α_k ,
- calculating the search direction \mathbf{u}_k .

Furthermore, gradient-based optimization algorithms share the following general form:

1. Start with an initial guess $\boldsymbol{\eta}_0$ of the solution $\boldsymbol{\eta}^*$
2. If the objective function φ at $\boldsymbol{\eta}_k$ is minimal, then stop.
3. Determine an improved estimate $\boldsymbol{\eta}_{k+1} = \boldsymbol{\eta}_k + \alpha_k \mathbf{u}_k$
4. go to 2.

More details can be found in Klose and Hielscher.²⁸

Gradient techniques differ mainly in the way the step length α_k and the search direction \mathbf{u}_k are calculated. In OT the most common method to determine the search direction has been the nonlinear conjugate gradient (CG) technique.^{15,21} We use the more complex quasi-Newton (QN) method that provides better reconstruction results.²⁸ Once the minimum is found, the final result is the distribution of the optical parameters. This method requires the gradient of the objective function, $d\varphi/d\mu_a^{x \rightarrow m}$ and $d\varphi/d\eta$, which is calculated by means of an adjoint differentiation technique.²³

3. RESULTS

In this work we demonstrate the feasibility of reconstructing the quantum yield η by means of the ERT applied to small geometries mimicking tissue-like media. We used synthetically generated measurement data due to better quantification of the original optical parameters. The original isotropically scattering medium had a size of $3 \text{ cm} \times 3 \text{ cm}$ with the optical parameters $\mu_s^x = 10 \text{ cm}^{-1}$ and $\mu_a^{x \rightarrow} = 0.1 \text{ cm}^{-1}$ at the excitation wavelength and $\mu_s^m = 10 \text{ cm}^{-1}$ and $\mu_a^m = 0.1 \text{ cm}^{-1}$ at the emission wavelength. Three fluorescent heterogeneities with a size of $0.5 \text{ cm} \times 0.5 \text{ cm}$ were embedded inside the medium. The heterogeneities had a fluorophore absorption of $\mu_a^{x \rightarrow m} = 0.3 \text{ cm}^{-1}$, but with different quantum yields, i.e. $\eta_1 = 0.08$, $\eta_2 = 0.05$, and $\eta_3 = 0.02$ (see figure (2)) due to an assumed quenching process. Twelve isotropic sources and 88 detectors were equally distributed around the circumference of the medium resulting in 1056 source-detector pairs. The light propagation, i.e. the radiance, ψ , and fluence, ϕ , was calculated on a 61×61 grid with a S_4 method for both the calculation of the synthetic measurements and the predicted detector readings within the reconstruction process.

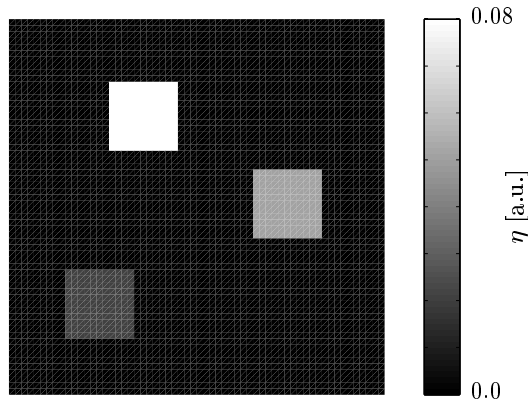


Figure 2. Original quantum yield distribution η .

The reconstruction process is divided into two steps. First, the fluorophore absorption $\mu_a^{x \rightarrow m}$ at the excitation wavelength λ_x was reconstructed by means of equation (3) starting from a homogeneous initial guess of $\mu_a^x = 0.1 \text{ cm}^{-1}$. Second, the reconstruction of η is performed by means of equation (4), where the reconstructed $\mu_a^{x \rightarrow m}$ distribution of the first step was assumed to be correct and was subsequently included in the source term $S^m = \frac{1}{4\pi} \eta \mu_a^{x \rightarrow m} \phi^x$. We started the reconstruction from an homogeneous initial guess of $\eta = 0.0001$ and terminated it after the relative difference $|(\varphi_{n+1} - \varphi_n)/\varphi_n|$ of subsequent iteration steps of the optimization process was smaller than $\xi = 5 \cdot 10^{-3}$. The reconstructed quantum yield η is shown in figure (3).

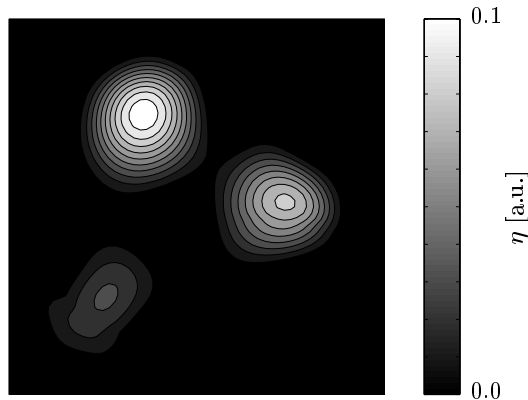


Figure 3. Reconstructed quantum yield distribution η .

The image of the quantum yield distribution shows a qualitatively and quantitatively accurate reconstruction of the fluorescent properties. All three heterogeneities are clearly visible. The maximum value of η of the upper heterogeneity is 0.09 and matches almost its original value of $\eta_1 = 0.08$. The maximum values of the other two heterogeneities are 0.056 and 0.023.

4. CONCLUSION

We have implemented the first image reconstruction code based on the equation of radiative transfer that can reconstruct fluorescent sources inside highly scattering tissue-like media. By not relying on the diffusion approximation, this algorithm promises to provide more accurate solutions in cases where the diffusion approximation fails, such as in media with small geometries or with high absorption coefficients. More detailed studies will be necessary to quantify the advantages of the presented code and to prove its usefulness in clinically relevant problems.

ACKNOWLEDGMENTS

This work was supported in part by a postdoctoral fellowship for Alexander D. Klose from the Ernst-Schering Research Foundation (Germany).

REFERENCES

1. R. Weissleder and U. Mahmood, "Molecular imaging," *Radiology* **219**(2), pp. 316–333, 2001.
2. J. R. Allport and R. Weissleder, "In vivo imaging of gene and cell therapies," *Exp. Hematology* **29**, pp. 1237–1246, 2001.
3. K. Licha, "Contrast agents for optical imaging," in *Topics in Current Chemistry*, pp. 1–29, Volume 222, Springer, Heidelberg, 2002.
4. J. R. Lakowicz, *Principles of Fluorescence Spectroscopy*, Plenum Press, New York, 1983.
5. D. Y. Paithankar, A. U. Chen, B. W. Pogue, M. S. Patterson, and E. M. Sevick-Muraca, "Imaging of fluorescent yield and lifetime from multiply scattered light reemitted from random media," *Appl. Opt.* **36**(10), pp. 2260–2272, 1997.
6. H. Jiang, "Frequency-domain fluorescent diffusion tomography: a finite-element-based algorithm and simulations," *Appl. Opt.* **37**(22), pp. 5337–5343, 1998.
7. J. Chang, H. L. Graber, and R. L. Barbour, "Luminescence optical tomography of dense scattering media," *J. Opt. Soc. Am. A* **14**(1), pp. 288–299, 1997.
8. R. Roy and E. M. Sevick-Muraca, "Truncated Newton's optimization scheme for absorption and fluorescence optical tomography: Part II reconstruction from synthetic measurements," *Opt. Exp.* **4**(10), pp. 372–382, 1999.
9. R. Roy and E. M. Sevick-Muraca, "A numerical study of gradient-based nonlinear optimization methods for contrast enhanced optical tomography," *Opt. Exp.* **9**(1), pp. 49–65, 2001.
10. J. Lee and E. Sevick-Muraca, "Fluorescence-enhanced absorption imaging using frequency-domain photon migration: tolerance to measurement error," *J. Biomed. Opt.* **6**(1), pp. 58–67, 2001.
11. J. Chang, H. L. Graber, and R. L. Barbour, "Imaging of fluorescence in highly scattering media" *IEEE Trans. Biomed. Eng.* **44**(9), pp. 810–822, 1997.
12. M. A. O'Leary, D. A. Boas, X. D. Li, B. Chance, and A. G. Yodh, "Fluorescence lifetime imaging in turbid media," *Opt. Lett.* **21**(2), pp. 158–160, 1996.
13. V. Ntziachristos and R. Weissleder, "Experimental three-dimensional fluorescence reconstruction of diffuse media by use of a normalized Born approximation," *Opt. Lett.* **26**(12), pp. 893–895, 2001.
14. S. R. Arridge and J. C. Hebden, "Optical imaging in medicine: II. Modeling and reconstruction," *Phys. Med. Biol.* **42**, pp. 841–853, 1997.
15. S. R. Arridge, "Optical tomography in medical imaging," *Inv. Prob.* **15**, pp. R41–R93, 1999.
16. S. R. Arridge and M. Schweiger, "A general framework for iterative reconstruction algorithms in optical tomography, using a finite element method," in *Computational Radiology and Imaging: Therapy and Diagnostics. The IMA Volumes in Mathematics and its Applications*, Ch. Boergers and F. Natterer, ed., pp. 45–70, Springer, New York, 1999.
17. R. Aronson and N. Corngold, "Photon diffusion coefficient in an absorbing medium," *J. Opt. Soc. Am. A* **16**(5), pp. 1066–1071, 1999.
18. B. Chen, K. Stamnes, and J. J. Stamnes, "Validity of the diffusion approximation in bio-optical imaging," *Appl. Opt.* **40**(34), pp. 6356–6366, 2001.
19. A. D. Kim and A. Ishimaru, "Optical diffusion of continuous-wave, pulsed, and density waves in scattering media and comparisons with radiative transfer," *Appl. Opt.* **37** (22), pp. 5313–5319, 1998.
20. A. H. Hielscher, R. E. Alcouffe, and R. L. Barbour, "Comparison of finite-difference transport and diffusion calculations for photon migration in homogeneous and heterogeneous tissues," *Phys. Med. Biol.* **43**, pp. 1285–1302, 1998.
21. A. H. Hielscher, A. D. Klose, and K. M. Hanson, "Gradient-based iterative image reconstruction scheme for time-resolved optical tomography," *IEEE Trans. Med. Imag.* **18**(3), pp. 262–271, 1999.

22. A. D. Klose and A. H. Hielscher, "Iterative reconstruction scheme for optical tomography based on the equation of radiative transfer," *Med. Phys.* **26** (8), pp. 1698–1707, 1999.
23. A. D. Klose and A. H. Hielscher, "Optical tomography using the time-independent equation of radiative transfer. Part II: Inverse model," *J. Quant. Spectrosc. Radiat. Transf.* **72**(5), pp. 715–732, 2002.
24. J. J. Duderstadt and W. R. Martin, *Transport theory*, John Wiley & Sons, New York, 1979.
25. E. E. Lewis and W. F. Miller, *Computational Methods of Neutron Transport*, John Wiley & Sons, New York, 1984.
26. B. G. Carlson and K. D. Lathrop, "Transport Theory - The Method of Discrete Ordinates," in *Computing Methods in Reactor Physics*, H. Greenspan, ed., pp. 166–266, Gordon and Breach, New York, 1968.
27. A. D. Klose, U. Netz, J. Beuthan, and A. H. Hielscher, "Optical tomography using the time-independent equation of radiative transfer. Part I: Forward model," *J. Quant. Spectrosc. Radiat. Transfer* **72**(5), pp. 691–713, 2002.
28. A. D. Klose and A. H. Hielscher, "Quasi-Newton methods in optical tomographic image reconstruction," *Inv. Prob.*, in print, 2003.
29. S. G. Nash and A. Sofer, *Linear and nonlinear programming*, McGraw-Hill, New York, 1996.